NASA Technical Memorandum 104627

Degradation of FEP Thermal Control Materials Returned from the Hubble Space Telescope

Thomas M. Zuby, Kim K. de Groh, and Daniela C. Smith

DECEMBER 1995

NASA Technical Memorandum 104627

Degradation of FEP Thermal Control Materials Returned from the Hubble Space Telescope

Thomas M. Zuby
Unisys Government Systems Group
Lanham, Maryland

Kim K. de Groh
NASA Lewis Research Center
Cleveland, Ohio

Daniela C. Smith
Cleveland State University
Cleveland, Ohio

National Aeronautics and
Space Administration

Goddard Space Flight Center
Greenbelt, Maryland 20771

1995

This publication is available from the NASA Center for AeroSpace Information,
800 Elkridge Landing Road, Linthicum Heights, MD 21090-2934, (301) 621-0390.

DEGRADATION OF FEP THERMAL CONTROL MATERIALS RETURNED FROM THE HUBBLE SPACE TELESCOPE

Thomas M. Zuby
Unisys Government Systems Group
NASA Goddard Space Flight Center
Greenbelt, Maryland, 20771

Kim K. de Groh
NASA Lewis Research Center
Cleveland, Ohio, 44135

Daniela C. Smith
Cleveland State University
NASA Lewis Research Center
Cleveland, Ohio, 44135

ABSTRACT

After an initial 3.6 years of space flight, the Hubble Space Telescope (HST) was serviced through a joint effort with the National Aeronautics and Space Administration (NASA) and the European Space Agency (ESA). Multi-layer insulation (MLI) was retrieved from the electronics boxes of the two magnetic sensing systems (MSS), also called the magnetometers, and from the returned solar array (SA-I) drive arm assembly. The top layer of each MLI assembly is fluorinated ethylene propylene (FEP, a type of Teflon). Dramatic changes in material properties were observed when comparing areas of high solar fluence to areas of low solar fluence. Cross sectional analysis shows atomic oxygen (AO) erosion values of up to 25.4 μm (1 mil). Greater occurrences of through-thickness cracking and surface microcracking were observed in areas of high solar exposure. Atomic force microscopy (AFM) showed increases in surface microhardness measurements with increasing solar exposure. Decreases in FEP tensile strength and elongation were measured when compared to non-flight material. Erosion yield and tensile results are compared with FEP data from the Long Duration Exposure Facility (LDEF). AO erosion yield data, solar fluence values, contamination, micrometeoroid or debris (MMD) impact sites, and optical properties are presented.

INTRODUCTION

The HST was launched April 24, 1990, and was deployed April 25. The original orbital altitude was 614 km at an inclination of 28.5°. The HST was captured on Dec. 4, 1993, at an altitude of 587 km, serviced through a joint effort by NASA and ESA, and then released on December 10 at an altitude of 595 km. Prior to the first servicing mission, the telescope was exposed to spaceborne phenomena such as solar and AO fluence,

charged particles, and micrometeroid or orbital debris. A preliminary ram AO fluence of 7.59×10^{20} atoms/cm^2 has been calculated for the HST for the initial 3.6 years of spacecraft operation (Ref. 1).

The study of environmental degradation effects on materials is important because the extent of damage to materials such as thermal control surfaces is a concern for the durability of satellite systems. AO can chemically erode materials such as FEP. Ultraviolet radiation (UV) can embrittle polymers by chain scission and/or crosslinking. Thermal exposure can affect the rates at which AO erosion occurs (Ref. 2) and is believed to affect the rate at which UV damage happens. Electron and proton radiation can induce embrittlement and degradation in polymers also. MMD impacts typically cause very localized damage, and are generally not considered as big a threat as AO and UV effects.

Servicing of the HST after 3.6 years in the low Earth Orbit (LEO) provides a unique opportunity to study long term space effects on spacecraft materials. There have only been a few other opportunities for studying long term space effects on materials, such as the retrieval of the Long Duration Exposure Facility (LDEF) after 5.8 years in LEO, and systems retrieved from the Solar Maximum spacecraft. Most often environmental durability evaluation of spacecraft materials is based on short term space exposure such as Shuttle experiments and ground testing. The data obtained from the retrieved HST materials will provide an opportunity to supplement data obtained from LDEF. Due to differences in altitude and spacecraft orientation, the data may also provide more insight into the synergistic effects between AO and UV. The HST data, combined with LDEF data, will also be used to improve ground to in-space calibrations for more accurate in-space durability predictions based on ground testing. This paper discusses the effects of long term space exposure on the FEP thermal control materials that were retrieved from HST during the first servicing mission.

THERMAL CONTROL MATERIALS

Three sections of MLI were obtained from the HST and were studied by Goddard Space Flight Center (GSFC) and Lewis Research Center (LeRC). Two blanket assemblies came from the magnetometer electronics boxes. During the first HST servicing mission, new magnetometers were placed onto the older magnetometers during astronaut extra-vehicular activity (EVA). In order to complete this attachment, MLI from the older units had to be removed. These MLI sections were bagged and returned for evaluation. The third MLI section was removed from the SA-I drive arm at Kennedy Space Center (KSC) during the de-integration of the servicing mission hardware. Figure 1 shows the approximate positions of these MLI materials on the HST.

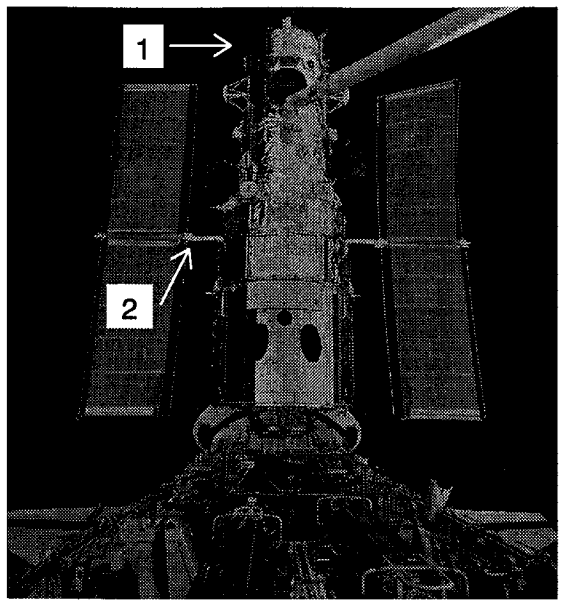

Figure 1: HST as it was being berthed in the cargo bay of the Endeavour Shuttle. Reference area 1 shows the approximate area in which the magnetometer MLI was removed. The magnetometers are on the opposite side of the telescope, and therefore cannot be seen from this angle. Reference area 2 shows the approximate area for the SA-I drive arm MLI assembly.

Magnetometer MLI

The magnetometer MLI is a sandwich construction of several layers of thermal control materials. The top most (and space exposed) layer is FEP. The back side of the FEP is coated with vapor deposited aluminum (VDA). Underneath the FEP material are layers of embossed Kapton which have both sides coated with VDA. The assembly is held together by selective placement of acrylic transfer adhesive film and stitching. Velcro was used to secure the MLI to the magnetometer. Figure 2 is a pre-flight photograph of a magnetometer unit, along with a description of the unit's orientation on the spacecraft. Figure 3 shows a photograph of the retreived magnetometer blankets. At the present time, it has not been determined from which MSS unit the corresponding MLI sections were removed. Markings or other identification are not present on the blankets which would aid in matching the blanket to the proper magnetometer unit.

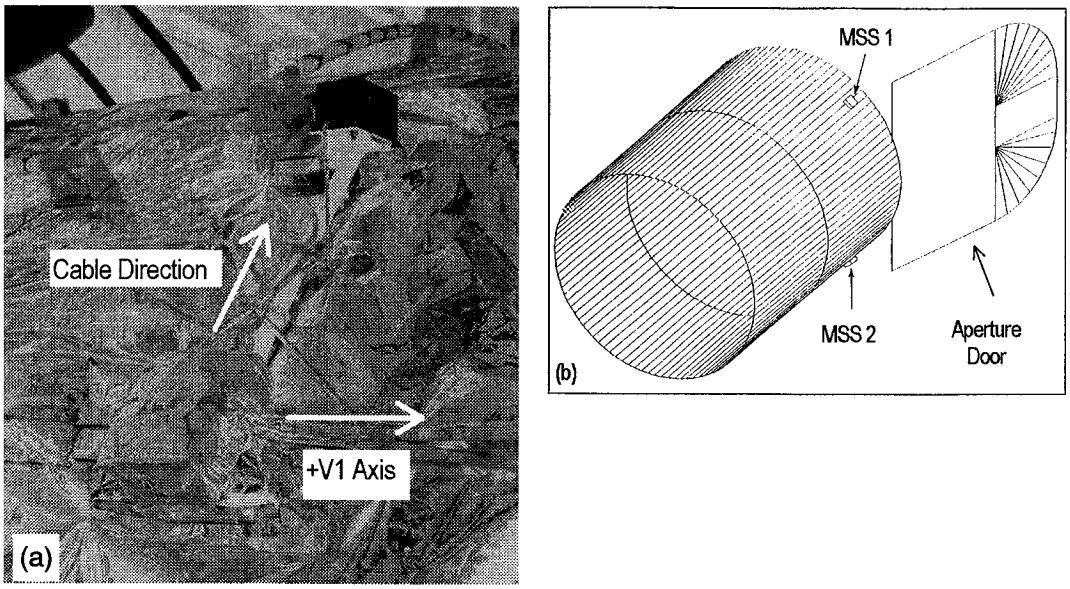

Figure 2: (a) Pre-flight photograph of MSS 2. To the right of this unit is the aperture door of the HST (+V1 direction). The area wrapped with the MLI is the electronics box. The area coated with black polyurethane paint is the sensor unit. Both units combined form the MSS. (b) A schematic representation of the location of the two magnetometer electronics boxes on the HST.

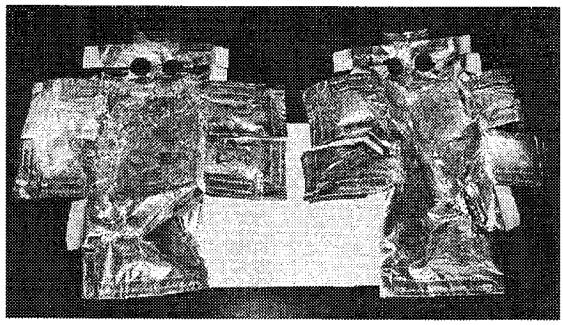

Figure 3: The returned magnetometer MLI assemblies. The thermal blankets are roughly 35 cm x 38 cm in size. The holes in the upper portion of the blankets are for cable access.

SA-I Drive Arm MLI

The SA-I MLI is also a sandwich construction of thermal control materials, with the top most layer being FEP. The back side of this FEP layer is coated with silver and Inconel. An acrylic transfer film adhesive is used to bond a fiber reinforced fabric to the metallized layer. Below the FEP/fabric sheet are alternating layers of double sided VDA perforated Kapton or Mylar sheet and polyester netting material. Stitching was used to hold this blanket assembly together. This MLI section wrapped around the circumference of the

drive arm assembly, and was secured by stitching the two joining edges. In total, four sections of MLI were wrapped around one drive arm assembly. Only one section was removed at KSC, and approximately one half of this blanket assembly was given to GSFC for analysis. Figure 4 shows the removal of the SA-I drive arm MLI at KSC.

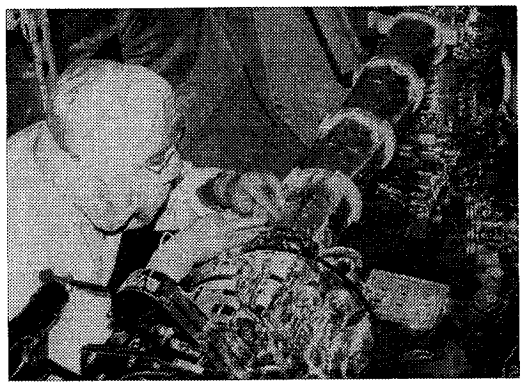

Figure 4: Lothar Gerlach, from the European Space Research and Technology Centre (ESTEC) is shown removing one of the SA-I drive arm MLI sections. The MLI is roughly 18 cm x 32 cm in size.

RESULTS

Preliminary MLI Inspection

Initial inspection of the MLI materials was performed in a class 100,000 cleanroom. All three blanket assemblies were noticeably affected by the space environment. Areas of both fairly clear reflectance and milky reflectance were apparent on each blanket assembly. Non-uniform areas of browning, and other areas of discoloration were noticed. Cracking of the FEP layer was evidenced by the presence of through-thickness cracks. The majority of discoloration and cracking was noticed on the surfaces with the highest solar fluence. Several MMD impact sites were also visible.

Rips or tears in the magnetometer MLI were also noticed. The blankets appear to have been torn in the removal process. The magnetometer blankets were secured by Velcro, and had to be tugged quite a bit to remove them.

After the initial inspections and photography were completed on the assemblies, one magnetometer MLI assembly, and the SA-I drive arm MLI assembly were disassembled. Specific areas of interest were sectioned from the blanket assemblies for further study. The second magnetometer MLI currently remains intact.

Magnetometer MLI

Figure 5 shows a model from Reference 3 that was used to calculate the solar fluence values of the exposed surfaces of the magnetometer MLI assemblies.

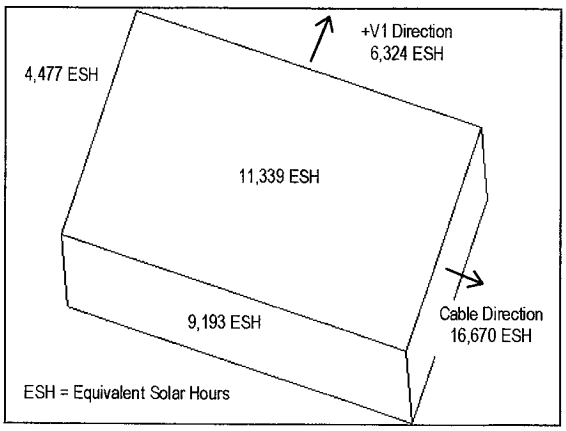

Figure 5: Calculated solar exposure values for the various sides of MSS 1 (see Fig. 2b). The cable direction is also referenced in Figure 2. The unit labeled MSS 2 would have similar ESH values, except the +V1 and -V1 directions (6,324 ESH and 9,193 ESH respectively) would be switched.

Both magnetometer MLI sections show a very dark discoloration in the areas of highest solar fluence. These dark areas appear in proximity to an underlying acrylic transfer film adhesive layer. The transfer adhesive is applied in 1.3 cm widths along the edges of the FEP layer. This is the approximate width of the darkened zone. The combination of thermal effects and UV induced degradation are thought to have caused this browning. Figure 6 shows the darkened areas for one of the two magnetometer MLI assemblies.

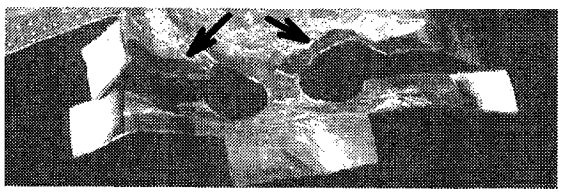

Figure 6: Solar induced browning of a magnetometer MLI. Acrylic tape is used in this area to fasten the top FEP layer to the second layer in this MLI assembly.

In addition to discoloration, areas of separation or peeling of the FEP film from the acrylic adhesive, and cracks in the FEP are apparent. The peeling and cracking are more pronounced on the surfaces of the magnetometer MLI with highest solar fluence. Figure 7 shows the peeling and cracking phenomena noticed in the cable areas of the FEP layer of the magnetometer MLI.

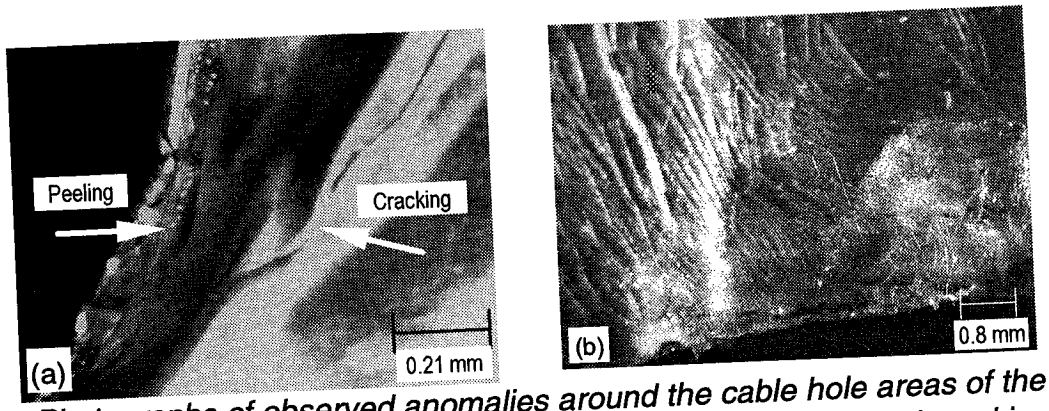

Figure 7: Photographs of observed anomalies around the cable hole areas of the magnetometer MLI. (a) Area of magnetometer MLI showing peeling and cracking of the FEP layer. (b) Area of the MLI surface showing severe cracking.

SA-I Drive Arm MLI

The overall appearance of this blanket assembly looked good except for the apparent browning of a silicone polymer used as a thread coating (see Fig. 8), and visible through-thickness cracks (see Fig. 9). A slight milky appearance was also present. These anomalies were noted in areas of high solar exposure. Modeling of the SA-I drive arm MLI to calculate solar exposure has not yet been performed. The cracks were noted at KSC during the de-integration of the hardware, before contact or any other handling was performed on the blanket assembly.

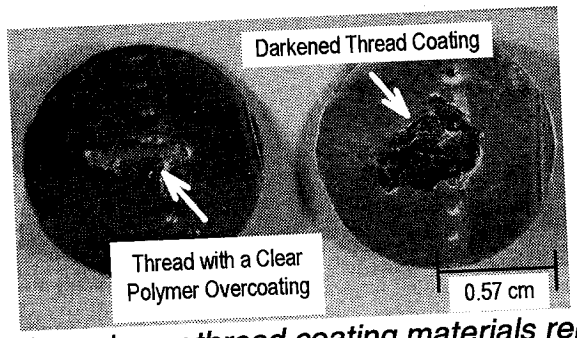

Figure 8: Comparison of the polymer thread coating materials removed from the SA-I MLI. The coating on the left is relatively undarkened, and the thread and MLI features are still visible. The coating on the right has darkened significantly. The thread is faintly visible through the coating. The sample on the left received a lower solar fluence than the sample on the right.

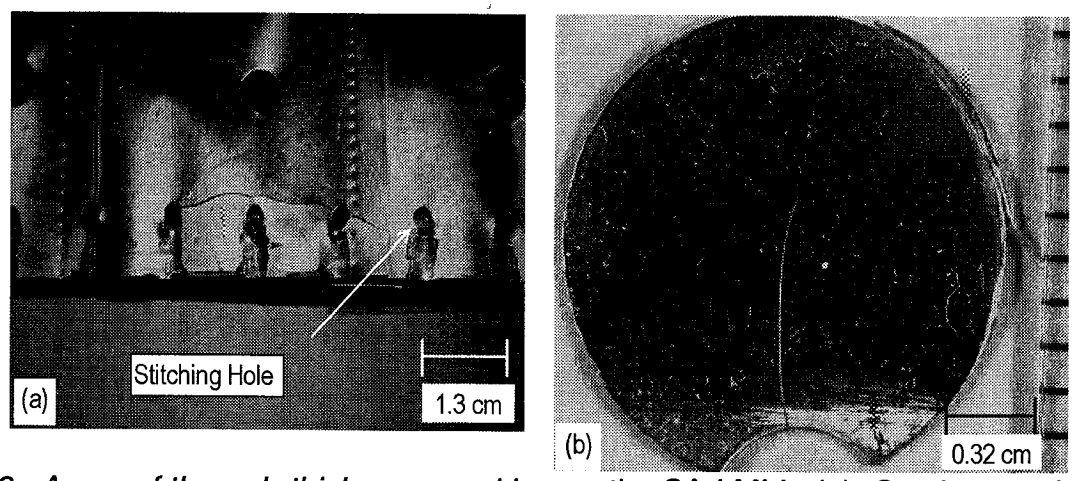

Figure 9: Areas of through-thickness cracking on the SA-I MLI. (a) Cracks are pictured near the edge of the blanket assembly. This is the area where the two mating sides were sewn together. (b) A cracked area sampled near one of the vent holes.

Contamination

Contamination analyses have been performed on samples from the SA-I MLI. Initial inspection noted specific areas of whitish, yellow, or brown discoloration. Figures 10 and 11 show various visible contamination aspects of selected areas of the SA-I MLI.

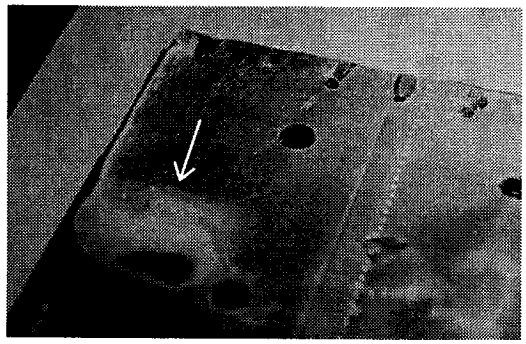

Figure 10: The largest localized area of contamination in the SA-I drive arm MLI is shown in this photograph.

XPS Results

Samples of the SA-I MLI were analyzed using x-ray photoelectron spectroscopy (XPS, Ref. 4). The instrument used in the analysis is a Surface Science Instrument M-Probe Spectrometer, which operates with monochromatic aluminum K-α x-rays. The overall results indicate that the areas of higher solar fluence have more occurrences of carbon-fluorine bond breakage and increased amounts of carbon-oxygen bonds. Fluorine was

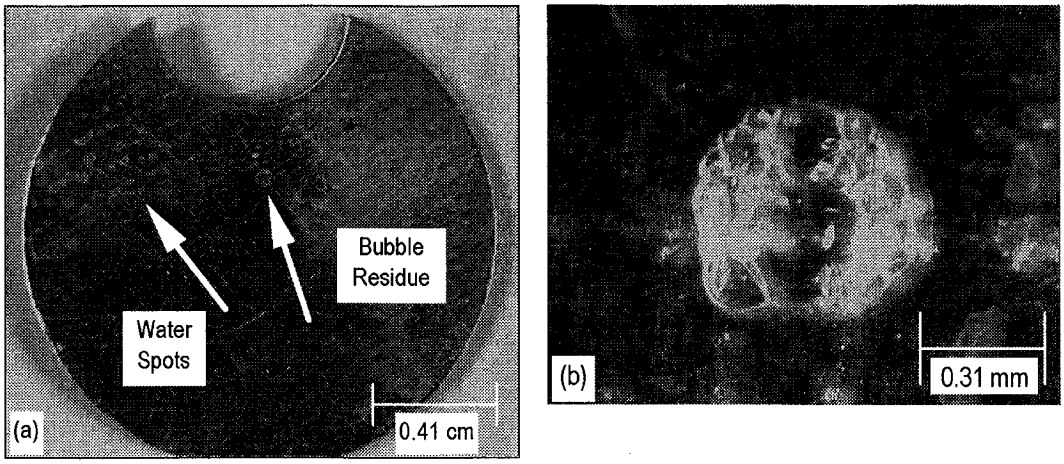

Figure 11: Indication of a pre-flight wiping operation is shown in these photographs. (a) Liquid droplet trails are evident in this picture leaving behind what is being termed "water spots". In proximity to the water spots, a bubble residue was located. (b) Enlargement of the bubble residue.

also found on unlikely areas such as silicone protective coatings, and on underlying MLI layers. In the pristine state, FEP material is strictly composed of carbon-carbon and carbon-fluorine bonds. These results indicate evidence that chemical reactions have occurred with AO and UV influence on the FEP surfaces. The mobility and deposition of the reacted FEP material on nearby surfaces, and the presence of silicone materials and their conversion to SiO_x through AO interaction is also observed.

Two vent hole areas showing through thickness cracks (similar to the crack of Figure 9b) were examined to see if chemical changes in the FEP material may have induced the cracking. The results vary between the two samples. For one sample, the analysis directly on the cracked area showed fragmented carbon-fluorine bonds, and less oxygen than an area adjacent to the cracked area. The second sample showed equivalent chemistry between cracked and uncracked areas.

Analysis of the large area of discoloration in Figure 10 showed the major constituent of the residue to be hydrocarbon based materials. This is the only area where hydrocarbons are predominant in the residue. Away from the center of the contaminated area, the FEP substrate, and small amounts of silicon and oxygen are present.

The darkened silicone thread protective material pictured on the right in Figure 8 was found to contain SiO_x and a small amount of fluorine. Adjacent to the polymer overcoat, the oxidized FEP substrate and trace amounts of silicon were found. The thread area itself contained only SiO_x and silicone.

In comparison, the sample with the clear thread coating (see Fig. 8) was analyzed. Adjacent to the coating, carbon, fluorine and a small amount of oxygen were noted. The clear coating was found to contain only silicon, carbon, and oxygen. No fluorine was detected. The oxygen content measured in the undarkened sample was considerably lower than that of the darkened sample.

The second layer of the SA-I drive arm MLI assembly was also sectioned and analyzed in two areas (see Figures 12a-b). The sample in Figure 12a was taken from an area exposed to the space environment below a vent hole in the top FEP layer. The sample in Figure 12b was taken below a stitching hole in the MLI assembly. The results from the XPS analysis show the presence of fluorine, silicone, and SiO_x on the VDA and Kapton surfaces.

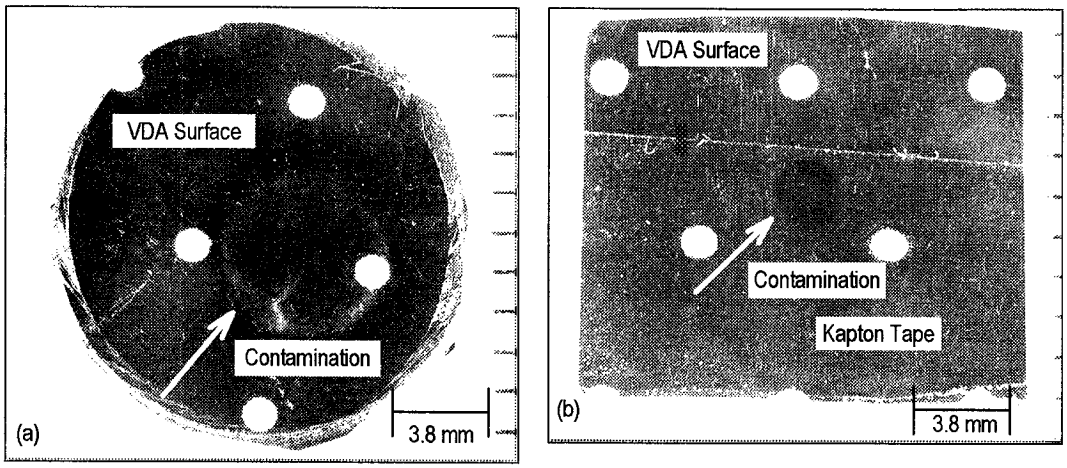

Figure 12: Second layer contamination from the SA-I MLI. The second layer is a Kapton substrate with both sides coated with VDA. The contaminants are predominantly fluorine, silicone and SiO_x. (a) This section was removed from underneath a vent hole in the FEP layer. (b) This sample was removed below a stitching hole (see Fig. 9a). The area of contamination is located on a piece of Kapton tape that has been applied to the VDA surface.

Micrometeoroid and Debris Impacts

Six MMD impact holes were found on the SA-I MLI. Examination was performed with optical microscopy up to 200x magnification. The largest "shock ring", or impact affected area was found on the solar facing surfaces of the MLI. Other samples were taken from material that was wrapped around the circular drive arm, and pointed away from the sun. It has not yet been determined if the shock ring size can be correlated to the embrittlement of the FEP material, or if is just a function of particle size. Figure 13 shows 4 of the 6 observed impact sites for the SA-I drive arm FEP layer. For the areas of high

solar exposure, the shock ring is over 7 times the diameter of the impact hole. For the areas of lower solar exposure, the shock ring is roughly 4.5 times the diameter of the impact hole.

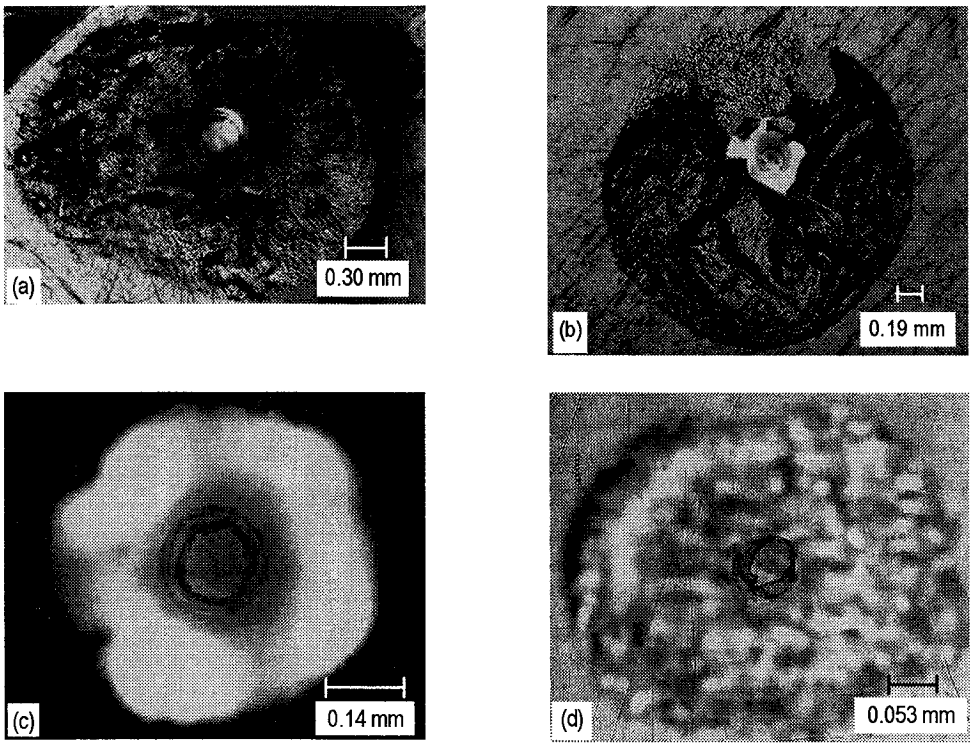

Figure 13: MMD impact sites from the FEP layer of the SA-I MLI. Samples (a) and (b) were removed from an area of the MLI that was predominantly solar facing. Sample (c) and (d) were removed from areas of lower solar fluence.

Physical Measurements

Atomic Force Microscope Microhardness Determination

Atomic force microscopy was used to measure the surface microhardness of magnetometer FEP surfaces. The instrument used is a Park Scientific Instruments AutoProbe Scanning Probe Microscope. An AFM measures the repulsive forces between atoms in a microscopic probe tip and in a sample surface. The tip is located at the end of a flexible cantilever. The sample surface is placed in contact with the probe tip using a piezo-electric scanner. The probe tip bends as the tip responds to the sample topography. A deflection sensor, utilizing a laser, monitors this bending and signals the sample scanner to move the sample up or down to keep the deflection constant. The up and down movement of the scanner, which matches the surface topography, is used to generate an image of the surface.

A force versus distance (f vs. d) curve can be generated on an AFM by plotting the vertical force on the cantilever tip (bending of the cantilever) as a function of the extension (or distance) of the piezoelectric scanner tube. For a surface with infinite hardness, the f vs. d curve would give a constant steep slope. Softer surfaces will have less steep and varying slopes as the probe sinks or pushes into the surface. By comparing the slopes of the tip deflection versus sample distance curves (f vs. d) for elastically deflected surfaces, relative surface microhardness can be determined.

Figure 14 shows preliminary results of AFM microhardness results for magnetometer MLI samples with various solar exposures. In this graph the force per distance ratio was plotted versus solar exposure. Because it is not known from which MSS unit the MLI pieces were removed, the data for 6,324 ESH and 9,193 ESH may be switched in this graph. As can be seen, there is an increase in surface hardness of FEP with increasing solar exposure. This hardness increase is believed to be primarily due to UV induced cross-linking of the FEP, which causes polymer embrittlement.

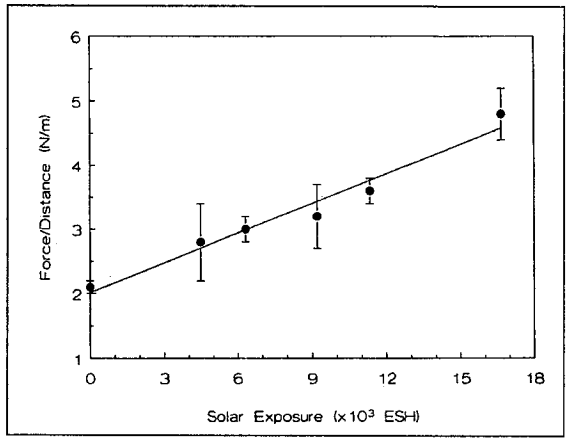

Figure 14: AFM microhardness results of the magnetometer MLI samples.

Tensile Measurements

The only FEP layer suited to perform tensile testing was material from the magnetometer MLI. The SA-I MLI could not be used because of the addition of the fiber reinforced fabric on the back of the FEP. Two dog bone shaped tensile specimens were taken from the magnetometer MLI FEP layer in the area that received 11,339 ESH. The die used to cut the samples was manufactured in accordance with American Society for Testing and Materials (ASTM) D1822, Type L (Ref. 5). The flight material is compared to stock material that was taken from the GSFC thermal blanket facility. The results indicate that changes in the mechanical properties have occurred. Minor decreases in yield strength (σ_{yield}) are noted. More significant changes are noted in the ultimate tensile strength (σ_{UTS}) and elongation values, where the properties have dropped by approximately 50% when compared to reference material. Table 1 lists the tensile values obtained from the magnetometer MLI.

Table 1: Tensile Values for the 11,339 ESH Section of the Magnetometer MLI

Sample ID	σ_{yield} (MPa)	σ_{UTS} (MPa)	Elongation, %, Relative to the Reference Material
Stock Material	14.6	27.2	100
Sample 1	13.6	15.7	57
Sample 2	13.6	13.6	33

Bending Tests

A two step bending process was another method used to evaluate the extent of embrittlement of the SA-I MLI FEP material. Small sections, roughly 2 cm on each side, were cut from the FEP layer. The samples were subjected to folding, or bending around an 0.83 mm diameter mandrel. In one direction, across the middle of the samples, bending was performed to cause compression on the space exposed surface of the FEP layer. Perpendicular to the compressive fold line, the FEP was bent so that the space exposed surface was subject to tensile stress. Each fold direction was subject to 25 cycles. The results indicate that compressive folding had no observed effect on the materials. Tensile folding induced cracking in the material for the samples with high solar exposure (see Fig. 15). No cracking was observed for the samples with the lower solar exposures.

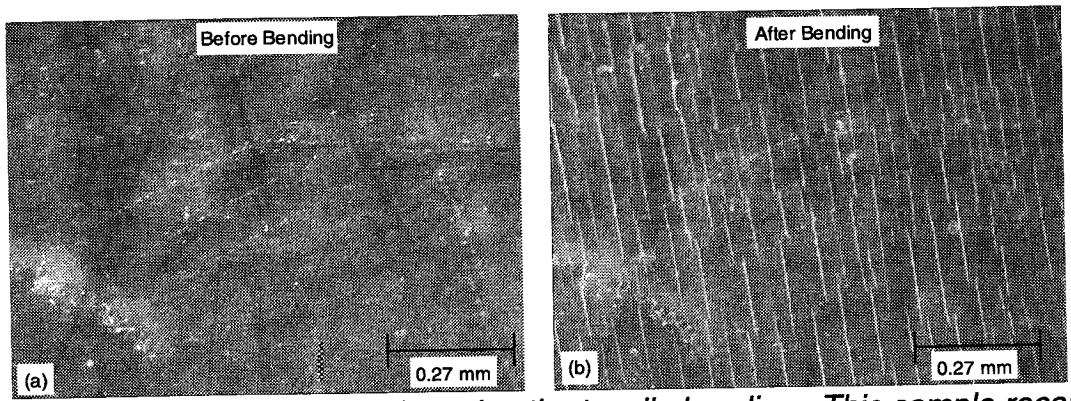

Figure 15: SA-I MLI FEP layer subjected to the tensile bending. This sample received the highest solar exposure. (a) Sample prior to bending. (b) Sample after the tensile bending.

Cross Sectional Thickness

Thickness calculations were performed using standard metallographic cross sectional techniques for both the magnetometer and the SA-I drive arm MLI materials. The samples were cut, mounted in an epoxy material, polished, and then measured (up to 800x magnification). The FEP samples are thinner for the areas of higher solar exposure when compared to the areas with lower solar exposure. The cross sectioning technique also showed an abundance of cracks for the high solar fluence areas. Figures 16 and 17 show cross sectioned samples from the magnetometer and SA-I MLI respectively. Figure 18 describes the locations of the samples removed from the SA-I MLI for the cross sectional thickness measurement. Tables 2 and 3 list the measured thickness values.

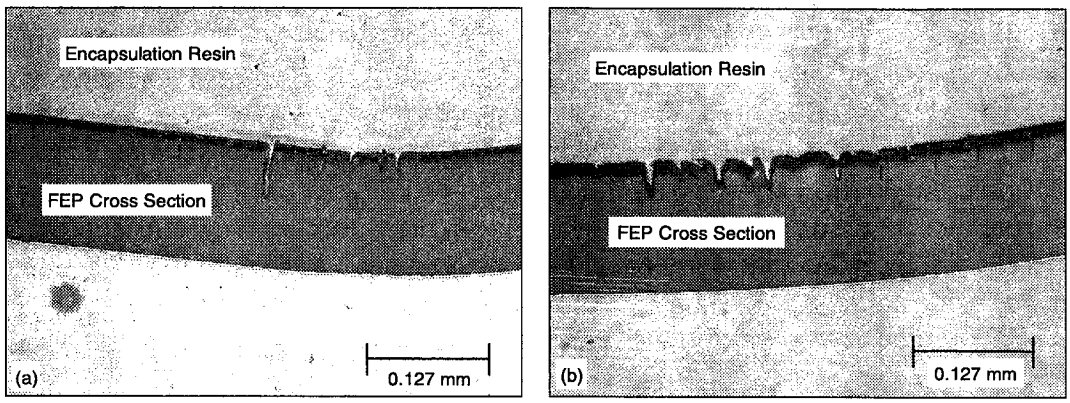

Figure 16: Cross sectional micrograph of the magnetometer FEP. Both thicknesses are measured to be 0.113 mm. (a) Sample removed from 11,339 ESH area of MLI, adjacent to the 16,670 ESH area. (b) Sample removed from the 16,670 ESH surface of the MLI.

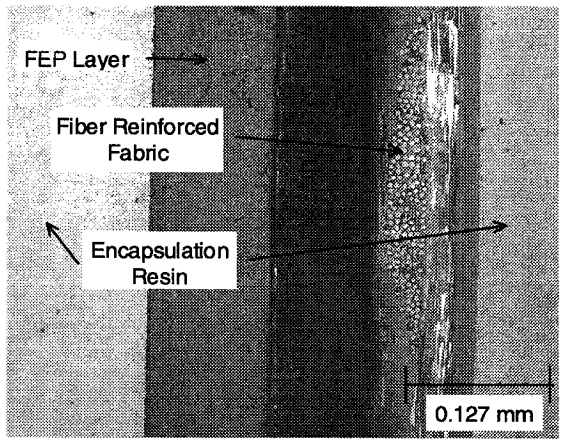

Figure 17: Cross section of the SA-I MLI FEP layer from an area of high solar exposure.

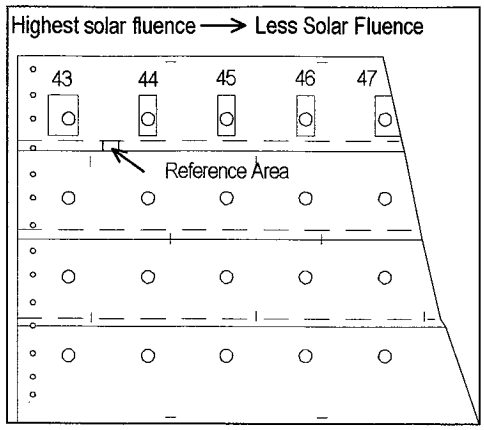

Figure 18: SA-I MLI thickness sample sectioning diagram. Samples 43-47 were taken to examine the material thickness as a function of varying amount of solar exposure. The reference sample was taken from underneath an overlapping piece of FEP, and was not directly exposed to the space environment.

Table 2: Magnetometer MLI FEP Layer Thickness Measurements

Solar Exposure, ESH	Thickness (mm)	Thickness Loss (mm)
16,670	0.113	0.024
11,339	0.113-0.134	0.003-0.024
9,193 or 6,324	0.132-0.138	0-0.005
6,324 or 9,139	0.133-0.137	0-0.004
4,477	0.129-0.136	0.001-0.008
0	0.137	0

Table 3: Thickness Measurements for the SA-I MLI Sample

Sample Number	Thickness (mm)	Thickness Loss (mm)
43	0.107	0.023
44	0.117	0.013
45	0.124	0.006
46	0.119	0.011
47	0.119	0.011
Reference	0.130	0

The 9,193 or 6,324 ESH values from Table 2 are mentioned this way because the magnetometer and its corresponding blanket have not been determined. The MLI assemblies were mounted so that the "right" side of the one unit saw equivalent exposure as the "left" side of the other unit.

A range of values is noted for the majority of samples thickness listed in Table 2. The ranges in thickness measurements may be caused by the attachment configuration of the blanket assembly. The MLI, as attached to the magnetometer electronics box (see Fig. 2a), does not leave as flat and orthogonal surfaces as the box used as the model for the calculation of solar fluence values (see Fig. 5). Various high spots and low spots appear on the surface of the MLI section. This geometry may lend to non-uniform exposure of the FEP material to the space environment. Secondly, silicone contamination on the FEP material could also protect the FEP from erosion.

A decrease in thickness loss is noted for sample 45 in Table 3. A cable bundle was located above this particular area, and is thought to have partially shaded the FEP material from the space environment. Disregarding the thickness measurement from Sample 45, a good correlation exists for increasing erosion with increasing solar exposure.

Crack Depth Measurement after Bending Evaluation

To evaluate the depth of embrittlement, the space exposed surface of the FEP samples from the SA-I drive arm MLI that were subject to tensile bending, were cross sectioned for crack depth measurement. Results show that the areas of high solar exposure exhibit deeper cracks than the areas of lower solar exposure. Three samples were removed from the SA-I MLI FEP layer. The samples (numbered 31, 32, and 33) were removed in proximity to thickness measurement samples 43 and 44 from Figure 18. Table 4 lists the crack depth data obtained from this test. The data was averaged from 13-16 measured cracks per sample. The largest tensile induced crack depth extended more than halfway through the FEP material indicating severe embrittlement of the solar facing surface.

Table 4: SA-I MLI FEP Layer Crack Depth Measurements after Tensile Bending

	Crack Depth (cm x10^{-3})		
	Sample 31	Sample 32	Sample 33
average value	2.40	1.50	1.01
maximum value	7.25	4.50	1.75
minimum value	1.00	0.25	0.50

Note: In order or relative solar exposure, sample 31 received the highest solar fluence of the three samples, and sample 33 the lowest.

Optical Properties

The solar absorptance (α_s) and normal emittance (ε_n) were measured for both the magnetometer and SA-I MLI samples (Ref. 6). When compared to reference literature measurements, the FEP layer from both blanket assemblies show increases in the values of α_s and ε_n. The magnetometer MLI shows larger variations and changes than the SA-I drive arm MLI. The α_s values were measured at ambient conditions using AV Technologies Laboratory Portable Spectral Reflectometer (LPSR). The reflectance was measured from 2500-250 nm at a 15° angle. The sample is mounted outside an integrating sphere, where α_s is calculated in accordance with ASTM E903 (Ref. 7). The ε_n values were measured also at ambient conditions, using a Gier Dunkle DB100 IR Reflectometer, integrated from 50-25 microns. Tables 5 and 6 list the optical properties for the magnetometer and the SA-I drive arm MLI FEP material respectively.

The values of 11,339 ESH referenced in Table 5 are distinguished by a superscript 1 and 2. The 1 value indicates the sample was removed adjacent to the 16,670 ESH surface. The 2 value sample was removed adjacent to the 4,477 ESH surface.

Table 5: Magnetometer MLI FEP Layer Optical Properties

ESH Value	α_s	ε_n
16,670	0.215	0.812
$11,339^1$	0.223	0.827
$11,339^2$	0.188	0.838
9,193, or 6,324	0.180	0.820
6,324, or 9,193	0.223	0.823
4,477	0.173	0.825
Literature Value(Ref. 8)	≤ 0.14	≥ 0.75
Literature Value(Ref. 9)	0.13	0.81

Table 6: SA-I drive arm MLI FEP Layer Optical Properties

ESH Value	α	ε_n
Highest	0.101	0.792
Middle Value	0.097	0.807
Lowest	0.102	0.803
Literature Value (Ref. 8)	≤ 0.09	≥ 0.75
Literature Value (Ref. 9)	0.08	0.81

Note: Because the ESH values for the areas of the SA-I MLI have not been calculated, only relative values, when compared to the solar pointing surface can be used.

AO AND UV AFFECTS

The data obtained from the MLI retrieved from the HST appear to be in agreement with sources that indicate that UV plays a strong role in AO erosion processes (Ref. 10) and FEP embrittlement (Ref. 11). For initial AO fluence calculations, the HST is considered to be a sweeping satellite, therefore, the maximum fluence values on any surface are calculated to be roughly $1/\pi$ of the ram value (7.59×10^{20} atoms/cm^2), or 2.4×10^{20} atoms/cm^2. Additional calculations for the particular surfaces of the MLI are in process, and therefore could not be included in this report. The actual AO fluence values for individual surfaces will likely differ from the $1/\pi$ value because of orientation and shading effects of the HST hardware.

A preliminary maximum erosion yield value of 1×10^{-23} cm^3/atom has been calculated using 2.4×10^{20} atoms/cm^2 as the AO fluence value. The maximum erosion yield can be calculated from either the magnetometer or the SA-I drive arm MLI, where maximum erosion values of $\approx$0.024 mm have been measured in the areas of highest solar fluence (see Tables 2-3). Other erosion yield values can then be determined from the FEP material using the measured thickness loss values. The various erosion thicknesses indicate a strong potential for synergy of increased AO erosion with increasing UV fluence.

COMPARISON TO LDEF RESULTS

LDEF results show that degradation occurs to the mechanical integrity of the FEP material. On average, a 30% loss in ultimate tensile strength and a 25% loss in elongation have been noted for silver backed FEP (Ref. 12), for all values of the solar and AO fluences received. The fluence values listed for the LDEF materials vary from 6,500-11,000 ESH and 10^6-10^{21} AO atoms/cm^2. In comparison, the HST results for VDA FEP material show an average decrease in ultimate tensile strength and relative elongation of 46% and 55% respectively for samples removed from the 11,339 ESH surface, with a maximum AO fluence of 2.4×10^{20} atoms/cm^2.

Samples of silver backed FEP removed from LDEF rows 7, 8, 10, and 11 have been analyzed for erosion yield (Ref. 12-13). Ram AO fluence values of 3.39×10^{21}-8.99×10^{21} atoms/cm^2 (Ref. 14) with solar fluence values of 7,111-10,680 (Ref. 15) ESH have been tabulated. After correction of the published erosion yield with updated fluence data, an average erosion yield of $\approx 3.4 \times 10^{-25}$ cm^3/atom has been calculated. A slight AO and UV dependence has also been reported. The preliminary HST erosion data shows over an order of magnitude higher erosion yield for the FEP layers exposed to the highest solar fluence, when compared to LDEF data (3.24×10^{-25} cm^3/atom for LDEF vs. 1×10^{-23} cm^3/atom for HST). These results are very unexpected and need further verification and explanation.

FUTURE PLANS FOR FEP TESTS

Additional research planned for the returned HST FEP materials includes calculation of actual solar and AO fluences on the various surfaces exposed to the space environment. Also, verification of erosion depths and erosion yields based on electron and atomic force microscopy will be performed. The extent of HST Teflon embrittlement will be compared with LDEF samples, with both surface hardness and tensile bending induced crack depth comparisons. Erosion yield and surface hardness data will also be compared to ground exposure data to improve ground to in-space correlation factors. Continued contamination evaluations and MMD studies are also planned.

CONCLUSIONS

Multilayer insulation samples retrieved from the HST during the first servicing mission have been analyzed for environmental degradation after 3.6 years of space exposure. Damage to the FEP layer of the MLI is most pronounced on the solar facing surfaces. Visible damage to the FEP includes surface and through-thickness cracking, discoloration and contamination.

Environmental exposure was found to greatly affect the physical properties of the FEP. AFM measurements show a trend of increasing surface microhardness with increasing solar exposure. Bending the FEP to induce tensile stresses in the surface was found to induce cracking for the higher solar fluence samples. Cracks extending more than half way through the thickness of the FEP were noted after bending for the samples with the highest solar fluence. Cracks were not induced in the samples with lower solar exposures. The ultimate yield strength and elongation to failure were found to have degraded by approximately 50% for samples exposed to 11,339 ESH as compared to non-flight material. Optical properties were found to have degraded also. The solar absorptance and normal emittance of VDA FEP from the magnetometer MLI increased by 43% and 3%, respectively, when compared to literature values. The solar absorptance of the silver backed FEP from the SA-I drive arm MLI increased by 11%, while the normal emittance essentially remained unchanged. Chemical analyses provide evidence of oxidation of the FEP and silicone materials located on the FEP. Teflon type residues were found on areas other than the FEP surfaces. Greater occurrences of chemical reactions and oxidation are noted on the solar facing surfaces, when compared to areas with lower solar fluence.

Additionally, for the highest solar fluence surfaces, cross sectional analyses shows erosion depths up to 23 and 24 μm for the SA-I and magnetometer MLI, respectively. Using the current estimated atomic oxygen fluence of 2.4×10^{20} atoms/cm^2, a maximum erosion yield of 1×10^{-23} cm^3/atom can be calculated. This unexpectedly high erosion yield is over an order of magnitude higher than erosion yields calculated for LDEF.

ACKNOWLEDGMENTS

The authors would like to thank the NASA-GSFC HST project office and ESA for providing the spacecraft thermal blanketing materials to perform the analyses, and to members of NASA-GSFC (Gloria Park for contamination analysis, Mike Viens for tensile measurements, and Patricia Friedberg for cross sectional thickness measurements), Todd Leonhardt of NYMA, Inc. for cross sectional preparation of samples for NASA LeRC, and Don Humes and Mark Kulick from NASA Langley Research Center for the initial MMD impact assessment.

REFERENCES

1. Rosecrans, G., *Atomic Oxygen Fluence on HST Prior to the December 1993 Servicing Mission*, Swales and Associates, Inc. for NASA-GSFC Code 724, March 10, 1994.

2. Gregory, J., *Interaction of Hyperthermal Atoms on Surfaces in Orbit: The University of Alabama Experiment*, Proceedings of the NASA Workshop on Atomic Oxygen Affects, Nov. 10-11, 1986, JPL 87-14, 1987, pp. 29-36.

3. Hitch, T., *MSS Flux Analysis*, Technical Note No. JT94-TN008, Jackson and Tull for NASA-GSFC Code 730, May 27, 1994.

4. Park, G., *XPS Analysis of HST SA-I Drive Arm MLI*, NASA-GSFC Code 313 memorandum, May 3, 1995.

5. ASTM D1822, *Standard Test Method for Tensile Impact-Energy to Break Plastics and Electrical Insulating Materials*, 1993.

6. Peters, W., *Recovered HST Aluminum Teflon and Silver Teflon Blanket Materials*, Swales and Associates, Inc. for NASA-GSFC Code 722, April 19, 1995.

7. ASTM E903, *Standard Test Method for Solar Absorptance, Reflectance, and Transmittance of Materials Using Integrated Spheres*, 1992.

8. Sheldahl, *Thermal Control Materials and Metallized Films, Part Number Listing and General Specifications*, 7/89, pp. 11, 15.

9. Henninger J., *Solar Absorptance and Thermal Emittance of Some Common Spacecraft Thermal-Control Coatings*, NASA RP 1121, April 1984.

10. Koontz S., et al, *Vacuum Ultraviolet Radiation/Atomic Oxygen Synergism in Materials Reactivity*, J. Spacecraft, Engineering Notes, Vol. 27, No. 3, May-June 1990, pp. 346-348.

11. Brinza D., et al, Vacuum Ultraviolet (VUV) Induced Degradation of Fluorinated Ethylene Propylene (FEP) Teflon Aboard the Long Duration Exposure Facility (LDEF), LDEF-69 Months in Space, First Post-Retrieval Symposium, NASA Conference Publication 3134 Part 2, June 1991, pp. 817-830

12. Rousslang K., et al, *Results of Examination of Silvered Teflon from the Long Duration Exposure Facility*, LDEF-69 Months in Space, First Post-Retrieval Symposium, NASA Conference Publication 3134 Part 2, June 1991, pp. 848, 852.

13. Banks B., et al, *Atomic Oxygen Interactions with FEP Teflon and Silicones on LDEF*, LDEF-69 Months in Space, First Post-Retrieval Symposium, NASA Conference Publication 3134 Part 2, June 1991, pp. 813.

14. Stein B., *LDEF Materials Overview*, , LDEF-69 Months in Space, Second Post-Retrieval Symposium, NASA Conference Publication 3194 Part 3, June 1992, pp. 775.

15. Bourassa, et al, *Solar Exposure of LDEF Experiment Trays*, NASA Contractor Report 189554, Boeing Defense and Space Group, February 1992, pp. A214-A215.

REPORT DOCUMENTATION PAGE

Form Approved
OMB No. 0704-0188

1. AGENCY USE ONLY *(Leave blank)*	2. REPORT DATE	3. REPORT TYPE AND DATES COVERED
	December 1995	Technical Memorandum

4. TITLE AND SUBTITLE

Degradation of FEP Thermal Control Materials Returned from the Hubble Space Telescope

5. FUNDING NUMBERS

Code 313

6. AUTHOR(S)

Thomas M. Zuby, Kim K. de Groh, and Daniela C. Smith

7. PERFORMING ORGANIZATION NAME(S) AND ADDRESS(ES)

Goddard Space Flight Center
Greenbelt, Maryland 20771

8. PERFORMING ORGANIZATION REPORT NUMBER

96B00024

9. SPONSORING/MONITORING AGENCY NAME(S) AND ADDRESS(ES)

NASA Aeronautics and Space Administration
Washington, D.C. 20546-0001

10. SPONSORING/MONITORING AGENCY REPORT NUMBER

TM-104627

11. SUPPLEMENTARY NOTES

Thomas M. Zuby: Unisys Government Systems Group, Lanham, Maryland; Kim K. de Groh: NASA Lewis Research Center, Cleveland, Ohio; Daniela C. Smith: Cleveland State University, Cleveland, Ohio

12a. DISTRIBUTION/AVAILABILITY STATEMENT

Unclassified-Unlimited
Subject Category: 23
Report available from the NASA Center for AeroSpace Information,
800 Elkridge Landing Road, Linthicum Heights, MD 21090; (301) 621-0390.

12b. DISTRIBUTION CODE

13. ABSTRACT *(Maximum 200 words)*

After an initial 3.6 years of space flight, the Hubble Space Telescope was serviced through a joint effort with the NASA and the European Space Agency. Multi-layer insulation (MLI) was retrieved from the electronics boxes of the two magnetic sensing systems (MSS), also called the magnetometers, and from the returned solar array (SA-I) drive arm assembly. The top layer of each MLI assembly is fluorinated ethylene propylene (FEP, a type of Teflon). Dramatic changes in material properties were observed when comparing areas of high solar fluence to areas of low solar fluence. Cross sectional analysis shows atomic oxygen (AO) erosion values up to 25.4 μm (1 mil). Greater occurrences of through-thickness cracking and surface microcracking were observed in areas of high solar exposure. Atomic force microscopy (AFM) showed increases in surface microhardness measurements with increasing solar exposure. Decreases in FEP tensile strength and elongation were measured when compared to non-flight material. Erosion yield and tensile results are compared with FEP data from the Long Duration Exposure Facility. AO erosion yield data, solar fluence values, contamination, micrometeoroid or debris impact sites, and optical properties are presented.

14. SUBJECT TERMS

Fluorinated Ethylene Propylene (FEP), Materials, Hubble Space Telescope

15. NUMBER OF PAGES

21

16. PRICE CODE

17. SECURITY CLASSIFICATION OF REPORT	18. SECURITY CLASSIFICATION OF THIS PAGE	19. SECURITY CLASSIFICATION OF ABSTRACT	20. LIMITATION OF ABSTRACT
Unclassified	Unclassified	Unclassified	Unlimited